



## Bioactivity-guided isolation of inositol as acetylcholinesterase inhibitory from endemic *Campanula baskilensis* Behçet: *In vitro* bioactivity, PCA analysis, and *in silico* supporting studies

Sarmad MARAH<sup>1</sup>, Yaşar IPEK<sup>2</sup>, Tevfik OZEN<sup>3</sup>, İbrahim DEMİRTAS<sup>4</sup>, Lutfi BEHCET<sup>5</sup>

<sup>1,3</sup>Ondokuz Mayıs University, Faculty of Science, Department of Chemistry, Samsun-Türkiye, <sup>2</sup>Department of Chemistry, Faculty of Science, Cankiri Karatekin University, Cankiri-Türkiye, <sup>4</sup>İğdır University, Faculty of Science and Art, Department of Biochemistry, İğdır-Türkiye, <sup>4</sup>Department of Pharmaceutical Chemistry, Faculty of Pharmacy, Ondokuz Mayıs University, Samsun, Türkiye, <sup>5</sup>Department of Biology, Bingöl University, Faculty of Science and Art, Bingöl-Türkiye

<sup>1</sup><https://orcid.org/0000-0001-6765-4605>, <sup>2</sup><https://orcid.org/0000-0002-1041-267X>, <sup>1,\*</sup><http://orcid.org/0000-0003-0133-5630>

<sup>3,4</sup><http://orcid.org/0000-0001-8946-647X>, <sup>5</sup><https://orcid.org/0000-0001-8334-7816>

✉: [tevfikoz@omu.edu.tr](mailto:tevfikoz@omu.edu.tr)

### ABSTRACT

This study aimed to identify the bioactivity-guided molecule in the fractions of *Campanula baskilensis* leaf methanol: chloroform extract. The bioactivity of leaf fractions was investigated to assess and isolate bioactive molecule/molecules and structural configurations. Fractionation and isolation processes were done using advanced column chromatography techniques. *In-vitro* bioactivity tests were applied, including enzyme inhibition, antibacterial, and DNA protection activities. The isolated compound was characterized using the NMR technique. *In silico* analyses were investigated using molecular docking, molecular dynamics, and final-state free energy calculations. 14 different fractions were obtained (F1-F14) through the fractionation. F12 has the highest AChE inhibition (IC<sub>50</sub>; 6.97±2.90 µg/mL), F6 has significant inhibition against carbonic anhydrase and α-amylase (IC<sub>50</sub>; 5.61±0.01 and 18.82±1.48 µg/mL). F12 and F11 have the highest antibacterial activity against *E. coli* (15.40±1.10 and 13.00±0.80 mm). F12 and F5 fractions have the highest protection activity in plasmid DNA, and F6 has the highest deoxyribose protection activity. Many fractions have high and varied bioactivity due to the bioactive compound components, as in F12. Principal component analysis showed that F12 positively correlated with the high inhibition activity for several bacteria and enzymes and high DNA protection. Therefore, further fractionation was applied using Sephadex LH-20 with ethyl acetate:methanol: hexane (5:5:1) to F12. Inositol was isolated according to results from the obtained fraction; the molecule characterization was clarified using the H-NMR and C13-NMR spectra. Molecular docking results showed binding between inositol and AChE. Further, molecular dynamics results showed the stability of inositol-AChE within 100 nanoseconds, and the energy calculations (gmx-MMPBSA) showed the strength of this interaction.

### Biochemistry

### Research Article

### Article History

Received : 05.02.2025

Accepted : 10.04.2025

### Keywords

*Campanula baskilensis*

Bioactivity-guided isolation

*In vitro* bioactivity

*In silico* studies

Endemik *Campanula baskilensis* Behçet bitkisinden asetilkolinesteraz inhibitörü olarak inositolün biyoaktivite rehberliğinde izolasyonu: *In vitro* biyoaktivite, PCA analizi ve *In silico* destekleyici çalışmalar

### ÖZET

Bu çalışmada *Campanula baskilensis* yaprak metanol:kloroform ekstraktının fraksiyonlarında biyoaktivite-yönlendirmeli moleküle ulaşılması amaçlanmıştır. Biyoaktif molekül/moleküllere ve yapısal konfigürasyona ulaşmak ve izole etmek için yaprak fraksiyonlarının biyoaktivitesi araştırıldı. Fraksiyonlama ve izolasyon işlemleri gelişmiş kolon kromatografisi tekniği kullanılarak gerçekleştirildi. Fraksiyon örnekleri için enzim inhibisyonu, antibakteriyel ve DNA koruma aktiviteler dahil üzere *in vitro* biyoaktivite testleri uygulandı. İzole edilen bileşik NMR tekniği kullanılarak karakterize edildi. *In silico* analizlerle moleküler doking, moleküler dinamikler ve

### Biyokimya

### Araştırma Makalesi

### Makale Tarihçesi

Geliş Tarihi : 05.02.2025

Kabul Tarihi : 10.04.2025

### Anahtar Kelimeler

*Campanula baskilensis*

Biyoaktivite rehberliğinde

son durum serbest enerji hesaplamalarını araştırıldı. Fraksiyonlama işlemi sonucunda 14 farklı fraksiyon elde edildi (F1-F14). F12 AChE karşı (IC<sub>50</sub>: 6.97±2.90 µg/mL), F6 karbonik anhidraz ve α-amilaza karşı (IC<sub>50</sub>: 5.61±0.01 ve 18.82±1.48 µg/mL) yüksek inhibisyon aktivite gösterdi. F12 ve F11 *E. coli*ye karşı en yüksek antibakteriyel aktivite gösterdi (15.40±1.10 ve 13.00±0.80 mm). F12 ve F5 fraksiyonları plazmit DNA'sında en yüksek koruma aktivitesine sahiptir ve F6, deoksiribozu korumak için en yüksek aktiviteye sahiptir. Birçok fraksiyonun, F12'de olduğu gibi, yüksek biyoaktif bileşikler içerdiğinden yüksek ve çeşitli bir biyoaktiviteye sahip olduğu gösterilmiştir. F12'nin test edilen çeşitli bakteri ve enzimler için yüksek inhibisyon aktivitesinin yanı sıra yüksek DNA koruması ile ana bileşen analizi pozitif korelasyon gösterdiği. Bu nedenle F12'ye Sephadex LH-20 ve etil asetat:metanol:hekzan (5:5:1) kullanılarak daha ileri fraksiyonlama ilerletildi. F12'den inositol izole edildi ve karakterizasyonu H-NMR ve C13-NMR spektrumları kullanılarak açıklandı. Moleküler doking sonuçlarına göre inositolün AChE enzimine bağlanabileceğini gösterdi. Ayrıca, moleküler dinamik sonuçları inositol-AChE'nin 100 nanosaniye içinde kararlı olduğunu gösterdi ve enerji hesaplamaları (gmx-MMPBSA) bu etkileşimin gücünü gösterdi.

izolasyon  
*İn vitro* biyoaktivite  
*İn silico* çalışmalar

**Atf İçin :** Marah, S., İpek, Y., Özen, T., Demirtaş, İ., & Behçet, L (2025). Endemik *Campanula baskilensis* Behçet bitkisinden asetilkolinesteraz inhibitörü olarak inositolün biyoaktivite rehberliğinde izolasyonu: *İn vitro* biyoaktivite, PCA analizi ve *İn silico* destekleyici çalışmalar. *KSÜ Tarım ve Doğa Derg 28 (3)*, 717-735. DOI: 10.18016/ksutarimdog.vi.1632935

**To Cite:** Marah, S., İpek, Y., Özen, T., Demirtaş, İ., & Behçet, L Marah, S., İpek, Y., Özen, T., Demirtaş, İ., & Behçet, L (2025). Bioactivity-guided isolation of inositol as acetylcholinesterase inhibitory from endemic *Campanula baskilensis* Behçet: *In vitro* bioactivity, PCA analysis, and *silico* supporting studies. *KSU J. Agric Nat 28(3)*, 717-735. DOI: 10.18016/ksutarimdog.vi.1632935

## INTRODUCTION

Natural products have always been a significant and successful source of drugs (Harvey, 2000). Several previous studies have emphasized that the chemical components of plants performed exceptionally well in drug discovery and development (Newman and Cragg, 2016). Identifying and isolating novel chemical components with high biological activity from natural product sources has contributed significantly to the development of pharmacology. It can be used as a model for developing a new potential drug or improving the effectiveness of previously used drugs (Nastić et al., 2018).

Natural bioactive ingredients are abundant in plants, also known as Phytochemicals. Despite its abundance of plants, only a few have been isolated and identified (Singh and Chaudhuri, 2018). The primary reason for the biosynthesis of bioactive compounds is protection or attractional in most plants. In addition, it has a biological activity reflected in multiple ways on other organisms, which could have beneficial or harmful effects on human and animal health (Bernhoft, 2010). Phytochemical benefits can act as a substrate for biochemical reactions, a cofactor or inhibitor for enzymes, remove unwanted components in the intestine, an agonist and antagonist to the cell receptor, a toxic chemical scavenger, can positively affect beneficial gut microorganisms, and can be a growth inhibitor as an antibacterial factor.

Moreover, through laboratory tests, many studies have shown the effectiveness of these materials against various diseases such as cancer, cardiovascular disease, diabetes, ulcers, inflammation, infection, neurologic disease, and many other diseases (Dillard and German, 2000). The most important groups of dietary phytochemicals are phenolics, alkaloids, nitrogen-containing compounds, organosulfur compounds, phytosterols, and carotenoids. Phenolics and carotenoids are the most studied dietary phytochemical groups related to human health and well-being (Liu, 2004).

This process necessitates studying these chemical structures and biochemical effects to achieve the researchers' requirements and/or to comprehensively understand the natural products and their effective contents to keep up with modern biological research, drug discovery, and development. The traditionally established process to isolate bioactive plant compounds begins with identifying and preparing the plant's materials, commonly by drying them and then extracting them using various chemical solvents, depending on the polarity from lowest to highest (Sarker and Nahar, 2012). A characteristic model to isolate a pure chemical compound from its natural origin is bioactivity-

guided fractionation, based on step-by-step separation of extracted components based on variances in the physical and chemical properties and estimation of the bioactivity, followed by another round of separation and assaying (Malviya and Malviya, 2017). Using numerous separation technologies for the plant parts extracts, such as column chromatography, gives a crude bioactive compound (Bucar et al., 2013).

*Campanula* L. is the most comprehensive type of the Campanulaceae family. It comprises 420 sub-genus, most spread in the circumboreal area, southern Asia, and northern Mexico (Alcitepe, 2011; Lammers, 2007; Yildirim, 2018). *Campanula* species cover a variety of chemical compounds; flavonoids, phenolics, anthocyanins, polyethylene's, phenylpropanoids, essential oils, acylated triterpenoids, glycosides, resins, coumarins, as well as wide range of subgroups of compounds; catechin, diosmin, quercetin, pelargonidin, delphinidin, cyanidin derivatives, fraxin, linalool,  $\alpha$ -terpineol, lavandulyl acetate, (E, E)-allo-ocimene (allo-ocimene),  $\beta$ -pinene,  $\alpha$ -cadinene,  $\beta$ -farnesene,  $\beta$ -caryophyllene, myo-inositol, lipids (glycolipids and phospholipids), fatty acid (Linoleic and oleic), sterols (stigmasterol and  $\beta$ -sitosterol), tocopherols ( $\alpha$ -tocopherol,  $\beta$ -tocopherol and  $\gamma$ -tocopherol) and alkaloids (Brandt et al., 2017; Dumlu et al., 2008; Hassanien et al., 2014; Ishida et al., 2008; Kim et al., 2017; Ouzounis et al., 2014; Vergauwen et al., 2000). *Campanula* secondary metabolites have numerous biological activities: antibacterial, antifungal, insecticidal, anticancer, and antioxidant potentials (Cuendet et al., 2001; Dumlu et al., 2008; Kim et al., 2006; Vincken et al., 2007). *Campanula* species have been used in traditional and oriental medicine for centuries. It has been used to reduce the risk of a wide range of respiratory diseases, including asthma, bronchitis, larynx inflammation, tonsillitis, pulmonary tuberculosis, and wart inflammation. It also has stimulating, antiallergic, antiphlogistic (anti-inflammatory drug), antioxidant, spasmolytic, antiviral, and antimicrobial properties and is used as an antiepileptic and constipation-regulating herb (Qi et al., 2020; Rameau et al., 1989).

In this previous study, *C. baskilensis* Behcet leaf part extract showed a higher biological activity than the other parts. This study aimed to achieve the active compounds through fractionation (Marah et al., 2024). For this purpose, we tested a wide range of bioactivity for each of the fractions of *C. baskilensis* including antibacterial (disc diffusion), enzyme inhibition (urease, acetylcholine esterase, butyrylcholine esterase, lipase, carbonic anhydrase,  $\alpha$ -amylase,  $\alpha$ -glucosidase and tyrosinase) activities and DNA damage protective capability all of the activities had been standardized and estimated using the standard materials. In addition to the spectroscopic examination H-NMR and C13-NMR to demonstrate the structure and chemical properties for the isolated molecules. Finally, we performed an *in silico* study to check the effectiveness of the isolated molecule by applying molecular docking, molecular dynamics, and energy calculations for the final state.

## MATERIAL and METHOD

### Plant material and chemicals

*Campanula baskilensis* Behcet sp. nov. is a locally endemic and distributed *Campanula* species known to be extended in the Baskil (Elazığ) district in the Eastern Anatolia territory of Turkey; 15 km south of Baskil town, 38° 27'18"N, 38° 49'41"E, southeast of Topalkem village, rocky area, 900–950 m a.s.l., gathered in July, L. Behçet 11860 (holotype: ANK, isotypes: Bingöl Univ. Herb. and Mustafa Kemal Univ. Herb.) by Prof. Dr. Lütüf Behçet, Bingöl University, Faculty of Arts, Department of Biology (Behçet and İlçim, 2018). All chemicals and reagent materials used are from pioneer companies: Sigma-Aldrich, Merck, Acros, Himedia, Thermoscientific, Gelentham, Isolab, and Carlo Erba.

### Fractionation and Isolation

This separation process was carried out on the sub-fractionation of the effective fractions in their antibacterial, enzyme inhibition, and DNA-related activities to reach the main pure compounds. The fractionation process was applied to the leaf part of *C. baskilensis* to obtain different fractions with different characteristics, and then isolate a pure compound from the plant. 251.00 grams of the leaf part of the plant was collected and dried in the shade at room temperature, completely ground via a laboratory blender, and ready for extraction, then the extraction done using the methanol-chloroform (MeOH: CHCl<sub>3</sub>, 1:1) solvent system by applying the maceration extraction method procedure three times in a row. Then, 32.00 g of extract was obtained by removing the solvent in the evaporator. The extract was impregnated with silica gel, eluted with hexane (Hex), and loaded onto the silica column. Also, chloroform, ethyl acetate (EA), and methanol solvents were used, respectively, according to the increasing polarity of the elution. With this crude fractionation, 14 main fractions were obtained. The fraction with high activity was treated with advanced chromatography using a Sephadex (LH-20) column in the methanol-ethyl acetate-hexane (5:5:1) solvent system to obtain the main components. The total number of fractions reached 14 (F1-F14) (Figure 2). This process was carried out the same way, using the Sephadex (LH-20) column until the pure compound in the leaf part of the *C. baskilensis* plant was reached. The molecular structure was determined using 1D and 2D NMR

techniques: H-NMR, C13-NMR, Heteronuclear Single Quantum Coherence (HSQC), Heteronuclear Multiple Bond Correlation (HMBC), and Correlated Spectroscopy (COSY).

### Enzyme inhibition activity

In the tests of the inhibitory ability of the *C. baskilensis* leaf fractions, we selected many enzymes whose abnormal activities may cause health problems and various human diseases. The first two enzymes associated with Alzheimer's disease, inhibition activity for the fraction's samples tested against cholinesterase's enzymes acetylcholine esterase (AChE) and butyrylcholine esterase (BChE), inhibition activity of the samples had been spectrophotometrically measured using the method by Ellman et al. (1961), based on the reaction of dithiobis(2-nitrobenzoic acid) (DTNB) reagent with thiocholine which will produce a yellow colored 5-thio-2-nitrobenzoate, which can be determined at 412 nm for both enzyme assays; After mixing 20 µL of the samples (8–1024 µg/mL), 140 µL of Na-K phosphate buffer (0.1 mM pH 8.0), 20 µL (3.3 mM) DTNB, and 20 µL of AChE or BChE (0.03 U/mL), the mixture was incubated for 15 minutes at 25 °C. After adding 10 µL of 1 mM butyrylcholine chloride or acetylcholine iodide, absorbance readings were determined at 412 nm. The results of the samples for inhibition activity were compared to galantamine as a positive control in both enzymes. The urease inhibition capacity for fractions and thiourea was determined spectrophotometrically based on a previously published method (Zhang et al., 2006), depending on the hydrolysis of urea in the presence of samples with a phenol-form), 25 µL of urease (5 U/mL, 100 mM Na-K buffer pH 8.2), 50 µL of urea (100 mM), and 10 µL fractions (8–1024 µg/mL) were mixed and incubated for 15 minutes at 30 °C. After that, 70 µL of alkaline reagent (2.5% NaOH + 4.7% NaOCl) and 45 µL of phenol (8% phenol + 0.1% sodium nitroprusside) were added, and the mixture was incubated for 50 minutes at 30 °C. The absorbance value was read at 630 nm.

The carbonic anhydrase (CA) inhibition activity for the fraction samples has been determined spectrophotometrically (Chanda et al., 2019), and acetazolamide was used as a positive control in this test. The basis of the experiment was the color shift of the enzyme-substrate *p*-nitrophenyl acetate (*p*-NPA) from transparent to yellow upon hydrolysis by the enzyme; 60 µL of the sample, 90 µL of 115 U/mL carbonic anhydrase (in 0.05 M pH 7.4 Tris-SO<sub>4</sub> buffer) was thoroughly mixed. The mixture was incubated for 15 minutes at 25 °C. After adding 60 µL of 10 mM *p*-NPA and 15 minutes at room temperature, the mixture's absorbance was determined at 400 nm.

The following two enzymes associated with diabetes mellitus are α-glucosidase and α-amylase. First, α-glucosidase inhibition activity was obtained using spectrophotometric methods (Mayur et al., 2010; Sancheti et al., 2010). As identical to the carbonic anhydrase inhibition test, inhibition activity determination for the fraction's samples against α-glucosidase enzyme was related to the color conversion of the enzyme-substrate *p*-nitrophenyl α-D-glucopyranoside (PNPG) from colorless to yellow-colored *p*-nitrophenol; 10 µL of the sample (8–1024 µg/mL), 25 µL of 0.2 U/mL enzyme, 25 µL of 0.5 mM PNPG, and 50 µL of 20 mM pH 6.9 phosphate buffer, 50 µL of 0.2 M NaCO<sub>3</sub> was added, and the combination was allowed to sit at 37 °C for half an hour. The absorbance of the mixture was then measured at 410 nm. α-amylase inhibition activity for the fraction samples was determined spectrophotometrically; A homogenous mixture of 82 µL of the sample (8–1024 µg/mL) and 10 µL of 1 U/mL α-amylase (20 mM PBS, pH 6.9) was made. After 10 minutes at 37 °C, 8 µL of substrate (1% starch) was added, and it was once more kept at 37 °C for 12 minutes. To halt the reaction, 50 µL of 10% HCl, 15 µL of iodine-KI (2.5 mM iodine (I<sub>2</sub>) + 6.5 mM KI (ddH<sub>2</sub>O)), and 50 µL of ddH<sub>2</sub>O were added. The mixture was then heated to a boil for 10 minutes, and once it cooled, absorbance values were taken at 620 nm. (Ercan and El, 2016), Depending on the color conversion in the test solution caused by the bonding of iodine reagent with the disaccharides produced by hydrolysis of starch by α-amylase in an acidic medium, absorbance values were measured at 620 nm. In both assays, acarbose was used as a positive control.

The lipase inhibition capacity for the fraction samples was determined using orlistat as a positive control based on a previously published method (McDougall et al., 2009; Trentin et al., 2020). The basis of the experiment was based on the color shift of the enzyme-substrate *p*-nitrophenyl octanoate (*p*-NPO) from transparent to yellow upon hydrolyzation by the enzyme, Samples of 20 µL (8–1024 µg/mL), 200 µL Tris-HCl buffer (100 mM Tris-HCl, pH 8.2), 20 µL 1 mg/mL lipase enzyme solution, and 20 µL 5.1 mM *p*-nitrophenyl octanoate were mixed homogeneously then incubated at 37 °C for 30 minutes, absorbance values were determined at 410 nm.

The last enzyme, tyrosinase, participates in melanin biosynthesis, and the inhibitory activity for the samples and the standard inhibitor kojic acid has been obtained based on a previously published method (Addar et al., 2019). The principle of this assay also depended on the color conversion made by the enzyme hydrolysis ability on the substrate (L-DOPA); 10 µL of sample, 150 µL of phosphate buffer (0.1 M, pH = 6.8), and 20 µL of tyrosinase enzyme (150 U/mL, 200 µg/mL), then incubated for 10 minutes at 37 °C. Next, 20 µL of 5 mM L-DOPA was added, and a reading was taken at 475 nm.

### Antibacterial Activity

*C. baskilensis* leaf fractions' antibacterial activity had been tested against two groups of bacteria: Three species of the gram-positive bacteria (*Staphylococcus aureus*, ATCC 25213; *Enterococcus faecalis*, ATCC 29212; and *Bacillus cereus*, CCM 99) and three species of the gram-negative bacteria (*Pseudomonas aeruginosa*, ATCC 15442; *Klebsiella pneumoniae*, ATCC 10031; and *Escherichia coli*, ATCC 25922). Tetracycline was used as a positive control in both tests.

The disc diffusion test, 1 mg/mL concentration of each fraction, was applied for the disc diffusion test based on a previously published method (Reller et al., 2009). 100 µL of 0.5 McFarland bacteria were spread on Mueller-Hinton agar placed in the petri dish, and then 40 µL of sample solution and positive control were absorbed with 6 mm discs and placed on the petri dish's surface. Results were measured in millimeters for the inhibition zones after 18 hours of incubation at 37 °C (except *B. cereus* incubated at 30 °C).

### DNA damage protection potential assays

*C. baskilensis* leaf fractions also had been tested for DNA protective activities, as DNA protection activity; using agarose-gel electrophoresis of plasmid DNA (pBR322) based on the protocol published in past studies (Baiseitova et al., 2021; Russo et al., 2003; Sevgi et al., 2015; Tepe et al., 2011). Test done as follows: firstly, in an Eppendorf tube, we add 4 µL glycerol, 5 µL fractions solution (1 mg/mL), 3 µL of pBR322 plasmid DNA (172 ng/µL), and 1 µL of 30% H<sub>2</sub>O<sub>2</sub>, respectively. The previous step was followed by incubation under UV radiation for 5 minutes at 25 °C. The Final step of preparing the solution for the test mixture was to add 2 µL of color indicator (bromophenol blue) to the test tubes. After that, the test mixture was carefully loaded into the agarose gel wells (1.5 % prepared by mixing 1X Tris-Borate-EDTA buffer and 2 µL of ethidium bromide). Then, electrophoresis was applied for 120 minutes at 90 volts. Results of the % DNA protective activity for the fractions calculated using the ImageJ program for UV transilluminator on the recorded gel image.

### Molecular Docking and Molecular Dynamics Evaluation

Due to the high biological activity of F12, especially in the AChE inhibition, we tested this molecule against the acetylcholinesterase crystal structure (PDB code: 1C2O). Molecular docking has been applied using the open-source software Auto Dock Vina (Trott and Olson, 2010). Using the optimized compound structures, we applied the docking with the target protein X-ray crystal structures with a high resolution from the PDB bank (Berman et al., 2000). The docking experiments maintained both the protein and compound in a flexible state. The free-binding affinities of the conformations binding to the active pockets of each protein, along with their interactions, were analyzed using DiscoveryStudio visualization software (BIOVIA, 2017).

The stability of the inositol-AChE resulting from docking was examined by GROMACS (Abraham et al., 2015). The CHARMM force field was applied to form the AChE force field, and then the complex was solvated with TIP3P water.

To balance the system's overall potential, Na<sup>+</sup> and Cl<sup>-</sup> ions were included. Subsequently, the steepest descent method, which involved 50,000 steps, was employed to minimize energy consumption. After that, NVT/NPT set the system's temperature and pressure to 310 K and 100 kPa, respectively. Ultimately, the MD simulation took 100 ns to complete (Bjelkmar et al., 2010). The results of the molecular dynamics simulation were analyzed by generating ligand hydrogen bond plots using Grace, along with assessments of RMSF (root mean square fluctuation), Rg (radius of gyration), and RMSD (root mean square deviation) (Akkoc et al., 2023; Başar et al., 2024).

The Molecular Mechanics/Poisson-Boltzmann surface area (MM/PBSA) was applied to achieve the binding-free energy of the end time complex using gmx\_mmpbsa software (Valdés-Tresanco et al., 2021).

### Statistical Analysis

Statistical analysis was done for all test results for the *C. baskilensis* fraction samples using the SPSS 22.0 (Statistical Package for the Social Sciences) package program. The test was conducted to find out the difference between the samples and between the samples with positive controls for all assays by applying the one-way ANOVA; nonparametric using the Kruskal-Wallis 1-way ANOVA (K samples), which reports statistically significant differences when p values ≤ 0.05 and the confidence interval is 95%, and the duplicate results values were performed as mean values ± standard deviation. Using the Minitab Biplot graph property, principal component analysis (PCA) was further applied to locate the variables that better differentiate between fractions.

## RESULTS and DISCUSSION

The results of enzyme inhibition capacity for the *C. baskilensis* leaf fractions were compared to the reference materials utilized to treat the health problems associated with an over-activity of enzymes under the same standard conditions for enzyme action. All the enzyme inhibition results for both fraction samples and the standard reference materials have been inserted in Table 1. The inhibition result of AChE showed F12 and F14 fractions to have the highest inhibition activity, while the F1 fraction showed the lowest inhibition activity among all fractions. Results also showed that F8, F12, and F14 have higher inhibition activity than galantamine. BChE inhibition results showed that the inhibition effects of the F4 and F10 fractions were very close to each other. At the same time, both fractions showed a maximal inhibition effect among all fractions. Also, F4 and F10 fractions proved their higher inhibition capacity than galantamine, a standard BChE inhibitor. The following two enzymes are urease and carbonic anhydrase. It is worth noting that *Campanula* and the other members of the *Campanulaceae* family have never been tested before for their inhibition activity against these two enzymes. For the urease enzyme, among all of the *C. baskilensis* fractions, the F7 fraction gave the maximal inhibitory effect; further, the F1, F2, F5, and F7 fractions' inhibitory effect was higher than thiourea. In the study conducted by Korkmaz et al. (2020), the effects of water, *n*-hexane, acetonitrile, and methanol extracts of *C. latifolia* on acetylcholinesterase inhibitory activity against galantamine were investigated. The resultant values (IC<sub>50</sub>) were found to be 532.03±0.64 µg/mL for water extract, 242.55±2.43 µg/mL for methanol extract, 100.94±3.59 µg/mL for acetonitrile extract, 295.42±0.33 µg/mL for *n*-hexane extract, and 10.48±0.09 µg/mL for galantamine. In this study, the acetylcholinesterase inhibitory activity was found to be higher in general.

Table 1. The enzyme inhibition activities of *C. baskilensis* fractions

*Çizelge 1. C. baskilensis fraksiyonlarının enzim inhibisyon aktiviteleri*

Samples	Activity, IC <sub>50</sub> (µg/mL)							
	AChE	BChE	Urease	CA	α-glucosidase	α-amylase	Lipase	Tyrosinase
F1	54.24±4.47 <sup>e</sup>	24.06±5.62 <sup>bcd</sup>	33.12±0.00 <sup>ab</sup>	181.45±1.34 <sup>j</sup>	99.28±2.93 <sup>e</sup>	73.72±2.17 <sup>e</sup>	98.66±1.16 <sup>f</sup>	36.28±4.48 <sup>bc</sup>
F2	31.24±0.37 <sup>d</sup>	4.85±1.27 <sup>a</sup>	34.05±3.60 <sup>ab</sup>	14.08±0.01 <sup>b</sup>	47.50±2.56 <sup>c</sup>	208.47±0.31 <sup>j</sup>	69.46±2.58 <sup>e</sup>	303.93±7.16 <sup>g</sup>
F3	32.64±3.07 <sup>d</sup>	81.00±0.64 <sup>e</sup>	42.52±0.00 <sup>bc</sup>	10.72±0.18 <sup>b</sup>	447.26±1.98 <sup>i</sup>	45.95±0.16 <sup>cd</sup>	56.29±4.04 <sup>de</sup>	33.91±1.90 <sup>bc</sup>
F4	11.32±0.80 <sup>ab</sup>	10.01±3.96 <sup>ab</sup>	70.94±3.90 <sup>ef</sup>	132.29±3.18 <sup>i</sup>	135.29±1.16 <sup>g</sup>	95.11±0.67 <sup>g</sup>	52.42±5.53 <sup>cd</sup>	58.98±0.87 <sup>de</sup>
F5	20.71±4.84 <sup>bcd</sup>	8.74±4.87 <sup>ab</sup>	21.91±2.58 <sup>a</sup>	78.57±2.42 <sup>g</sup>	38.60±1.79 <sup>abc</sup>	34.55±0.70 <sup>b</sup>	32.99±1.02 <sup>b</sup>	93.91±7.88 <sup>f</sup>
F6	30.16±3.02 <sup>d</sup>	16.70±5.51 <sup>abc</sup>	45.96±4.87 <sup>bc</sup>	5.61±0.01 <sup>ab</sup>	103.20±0.49 <sup>ef</sup>	18.82±1.48 <sup>a</sup>	53.36±0.96 <sup>cd</sup>	69.93±1.72 <sup>e</sup>
F7	25.67±3.02 <sup>cd</sup>	27.88±2.95 <sup>cd</sup>	20.96±1.23 <sup>a</sup>	53.28±0.75 <sup>f</sup>	44.05±1.75 <sup>bc</sup>	42.80±1.44 <sup>bc</sup>	69.58±5.03 <sup>e</sup>	36.37±5.76 <sup>bc</sup>
F8	7.90±0.05 <sup>ab</sup>	16.01±2.42 <sup>abc</sup>	383.75±0.00 <sup>h</sup>	35.22±1.14 <sup>cd</sup>	111.24±0.79 <sup>f</sup>	93.39±3.39 <sup>g</sup>	91.21±3.44 <sup>f</sup>	98.90±5.59 <sup>f</sup>
F9	9.23±6.96 <sup>ab</sup>	9.76±0.39 <sup>ab</sup>	47.01±1.66 <sup>bc</sup>	43.01±0.41 <sup>de</sup>	74.45±3.49 <sup>d</sup>	147.66±4.59 <sup>i</sup>	90.34±5.56 <sup>f</sup>	70.19±4.96 <sup>e</sup>
F10	14.30±4.23 <sup>abc</sup>	4.67±6.16 <sup>a</sup>	65.99±5.82 <sup>de</sup>	31.18±1.81 <sup>c</sup>	131.95±0.90 <sup>g</sup>	81.00±1.58 <sup>ef</sup>	35.83±2.96 <sup>b</sup>	96.28±4.54 <sup>f</sup>
F11	26.63±4.25 <sup>cd</sup>	32.91±5.21 <sup>d</sup>	40.24±1.12 <sup>bc</sup>	92.73±1.18 <sup>b</sup>	129.93±1.99 <sup>g</sup>	89.27±3.63 <sup>fg</sup>	92.10±4.53 <sup>f</sup>	24.66±3.48 <sup>ab</sup>
F12	6.97±2.90 <sup>a</sup>	33.38±2.65 <sup>d</sup>	86.91±4.39 <sup>g</sup>	54.04±0.91 <sup>f</sup>	36.78±0.26 <sup>ab</sup>	73.39±0.43 <sup>e</sup>	57.24±0.05 <sup>de</sup>	43.72±4.63 <sup>cd</sup>
F13	20.77±2.02 <sup>bcd</sup>	10.64±2.18 <sup>ab</sup>	84.73±7.48 <sup>fg</sup>	8.68±6.12 <sup>ab</sup>	47.31±2.46 <sup>c</sup>	72.08±3.34 <sup>e</sup>	26.07±4.23 <sup>b</sup>	23.15±4.34 <sup>ab</sup>
F14	6.06±1.29 <sup>a</sup>	10.59±5.04 <sup>ab</sup>	52.42±3.09 <sup>cd</sup>	47.90±3.57 <sup>ef</sup>	237.34±5.11 <sup>h</sup>	106.04±4.64 <sup>h</sup>	40.82±5.69 <sup>bc</sup>	55.64±5.24 <sup>de</sup>
Galantamine	8.03±0.68 <sup>ab</sup>	7.60±2.37 <sup>a</sup>	-	-	-	-	-	-
Thiourea	-	-	37.13±3.28 <sup>b</sup>	-	-	-	-	-
Acetazolamide	-	-	-	0.64±0.08 <sup>a</sup>	-	-	-	-
Acarbose	-	-	-	-	34.25±2.63 <sup>a</sup>	54.60±3.15 <sup>d</sup>	-	-
Orlistat	-	-	-	-	-	-	10.25±1.14 <sup>a</sup>	-
Kojic acid	-	-	-	-	-	-	-	7.85±0.65 <sup>a</sup>
P value	0.020	0.026	0.012	0.011	0.011	0.012	0.013	0.013

Values are mean±standard deviation; Different superscript letters (<sup>a-j</sup>) indicate significant differences in values within the same column ( $p \leq 0.05$ ), with a confidence interval of 95%.

On the other hand, looking at the inhibition results of the CA enzyme, F6 had a better inhibitory effect than other fractions; however, acetazolamide was the most efficient compared with the fraction samples. The following two enzymes that we tested are related to type 2 diabetes mellitus; therefore, researching compounds capable of determining their effectiveness is of excellent health importance. For the α-glucosidase inhibition activity, results determined that the F12 fraction from *C. baskilensis* leaf fractions has a higher inhibition effect compared to other fractions. In contrast, the F3 fraction has the lowest effect. Also, when the α-glucosidase inhibition level of F5 and F12 fractions was compared with other samples, it showed an inhibition effect close to the reference inhibitor molecule acarbose. The study conducted by Korkmaz et al. (2020) investigated the effects of water, acetonitrile, and methanol extracts of *C. latifolia* on α-glucosidase inhibitory activity against acarbose. The resultant values (IC<sub>50</sub>) were found to be 193.33±4.64 µg/mL for water extract, 30.42±1.04 µg/mL for methanol extract, 214.06±2.04 µg/mL for acetonitrile extract, and 35.03±0.22 µg/mL for acarbose. In this study, α-glucosidase inhibitory activity was higher. However, in the study conducted by Zarei and Tahazadeh (2020), the α-glucosidase inhibition activity

of the methanol extract of the *C. involucrata* plant was investigated, and the IC<sub>50</sub> value was found to be 20 µg/mL. It was determined that it had more effective α-glucosidase inhibition activity than this samples. On the other hand, the α-amylase inhibition test results showed that the inhibition activity of the F6 fraction of the *C. baskilensis* leaf fraction was more effective than that of other fractions. Among the *C. baskilensis* leaf fractions, the F2 fraction was found to have the lowest inhibitory activity. The activity of F3, F5, and F6 fractions showed a higher inhibition effect on α-amylase activity than acarbose. The inhibition activity results against the lipase enzyme showed that the F13 fraction was more effective than the other fractions in inhibiting the lipase enzyme activity. In the study carried out by Kim et al. (2011), α-amylase inhibition activities of water and ethanol extracts of *C. takesimana* Nakai and *Codonopsis lanceolata*, *Adenophora remotiflora*, *Asyneuma japonicum*, and *Adenophora triphylla* species belonging to the *Campanulaceae* family were compared with acarbose. In the study, 3.7±7.8% for *A. remotiflor* water extract, 3.9±7.5% for *C. takesimana* ethanol extract, 5.2±12.3% for *A. remotiflor* ethanol extract, 5.6±9.8% for *A. triphylla* ethanol extract, 14.6±7.9% for *A. japonicum* ethanol extract, and 80.15±0.23% for acarbose were found to have inhibitory effects. In this study, the inhibitory activities of fractions F3, F5, F6, and F7 gave higher effects compared to acarbose. Also, *C. takesimana*, *C. lanceolata*, *A. remotiflora*, *A. japonicum*, and *A. triphylla* samples were more effective compared to each other.

In contrast, the F1 fraction was found to have the lowest inhibitory activity among the fractions. Also, the results demonstrate that *C. baskilensis* leaf fractions have a lower inhibitory effect than orlistat. The last enzyme in this study was tyrosinase; the inhibitory activity of the tyrosinase enzyme was applied by comparing the *C. baskilensis* leaf fractions' activity results with the activity of the reference inhibitor material, kojic acid. As the results showed, the tyrosinase inhibition activity of the F13 fraction was found to be more effective than the other fractions, while the activity of the F2 fraction was found to have the lowest inhibitory effect; however, fractions were determined to have lower inhibition activity than kojic acid. The study conducted by Korkmaz et al. (2020) investigated the effects of water, n-hexane, acetonitrile, and methanol extracts of *C. latifolia* on tyrosinase inhibitory activity against kojic acid. The resultant values (IC<sub>50</sub>) were found to be 248.84±5.66 µg/mL for water extract, 226.91±3.27 µg/mL for methanol extract, 53.41±0.64 µg/mL for acetonitrile extract, 189.72±6.02 µg/mL for n-hexane extract and 32.58±0.27 µg/mL for kojic acid. In this study, the tyrosinase inhibitory activity was found to be higher for F1, F3, F7, F11, F12, and F13.

### Antibacterial activity

The antibacterial activity for the *C. baskilensis* leaf fractions was determined using a disc diffusion test to determine the bacterial growth inhibition as a zone in millimeters for the fractions in Table 2.

Table 2. Antibacterial activities of *C. baskilensis* fractions

Çizelge 2. *C. baskilensis* fraksiyonlarının antibakteriyel aktiviteleri

Antibacterial property	Sample	Gram-negative bacteria			Gram-positive bacteria		
		<i>E. coli</i>	<i>P. aeruginosa</i>	<i>K. pneumoniae</i>	<i>E. faecalis</i>	<i>B. cereus</i>	<i>S. aureus</i>
Inhibition zone, mm	F1	11.00±0.90	20.20±0.80	6.30±0.00	na	na	na
	F2	7.90±0.70	7.00±0.10	7.80±0.60	6.20±0.00	na	na
	F3	9.40±0.80	7.50±0.50	7.80±0.30	na	9.80±0.40	9.30±0.90
	F4	11.00±0.70	21.40±1.00	6.20±0.10	na	na	na
	F5	8.40±0.30	7.60±1.00	9.00±0.40	na	na	10.30±0.40
	F6	7.90±0.60	8.60±0.20	7.50±0.60	na	10.70±0.40	8.40±0.00
	F7	7.10±0.00	7.70±0.10	7.00±0.60	na	10.40±1.30	8.60±0.80
	F8	9.80±0.40	8.70±0.10	10.00±0.30	na	12.50±3.50	8.30±0.10
	F9	11.00±0.50	7.80±1.00	7.40±0.40	na	12.10±1.30	8.70±0.40
	F10	6.80±0.40	7.00±0.00	6.60±0.00	na	12.10±1.30	9.30±0.40
	F11	15.40±1.10	8.60±0.80	6.60±0.90	na	na	na
	F12	13.00±0.80	8.10±1.60	8.30±0.60	na	10.10±0.80	7.80±0.80
	F13	6.70±0.00	7.80±0.50	8.40±1.50	na	9.2±00.10	10.20±0.60
	F14	7.60±0.40	8.10±1.30	7.10±0.60	na	9.70±0.40	7.80±0.00
	Tetracycline		32.10±0.20	31.50±0.70	30.30±0.00	41.30±0.00	28.30±0.00

na: no activity

As the results of the disc diffusion test, firstly, for the gram-negative bacteria, against *E. coli*, F11 and F12 fractions gave the best inhibition effect among all fractions; however, tetracycline was more effective against *E. coli*. For the *P. aeruginosa*, inhibition zones for F1 and F4 fractions were at the top, yet tetracycline showed higher activity. Against *K. pneumoniae*, the most effective fractions were F8, F12, and F13, all of which had less activity than tetracycline. Also, we tested fraction samples against three gram-positive bacteria the fractions' growth inhibition activities were as follows: F2 fraction was the only fraction with an antibacterial effect against *E. faecalis*, yet its activity was lower than tetracycline activity. Against *B. cereus*, the F8 fraction showed the highest activity among the fractions. However, it was the nearest fraction in activity to tetracycline. Against *S. aureus*, the F13 fraction

was found to have the highest inhibition activity among all fractions; however, tetracycline was found to have a higher inhibition activity against *S. aureus* when compared with fraction results. In the study conducted by Sinek et al. (2012), the antibacterial activity of the essential oils of *C. glomerata* against various bacteria was investigated and the inhibition zones were found as 6 mm for *P. aeruginosa*, 10 mm for *S. aureus*, 8 mm for *E. faecalis* and 10 mm for *B. cereus*. When compared to this samples, most of them had higher effects.

### DNA related activities

The DNA-related activities tests aim to investigate the activity of protecting and preventing damage to DNA from reactive oxygen species and Ultraviolet (UV) radiation. *C. baskilensis* leaf fractions were investigated to determine protective effectiveness in protecting pBR322 plasmid DNA against UV radiation and oxidative stress (Figure 1). Agarose gel electrophoresis was applied to the *C. baskilensis* leaf fractions at 1 mg/mL. As both the agarose gel image and the chart of % plasmid DNA forms clarified, the results of protection activity for fractions were as follows: F12 followed by F5 fraction have the highest protection activity for the supercoiled form of plasmid DNA, while F11 has the lowest. On the other hand, F12, F2, and F3 fractions have the highest protection activity for the open-circular form of plasmid DNA, while F7 has the lowest effect. Among all fractions, the F11 fraction barely had a protection effect in both forms of plasmid DNA.

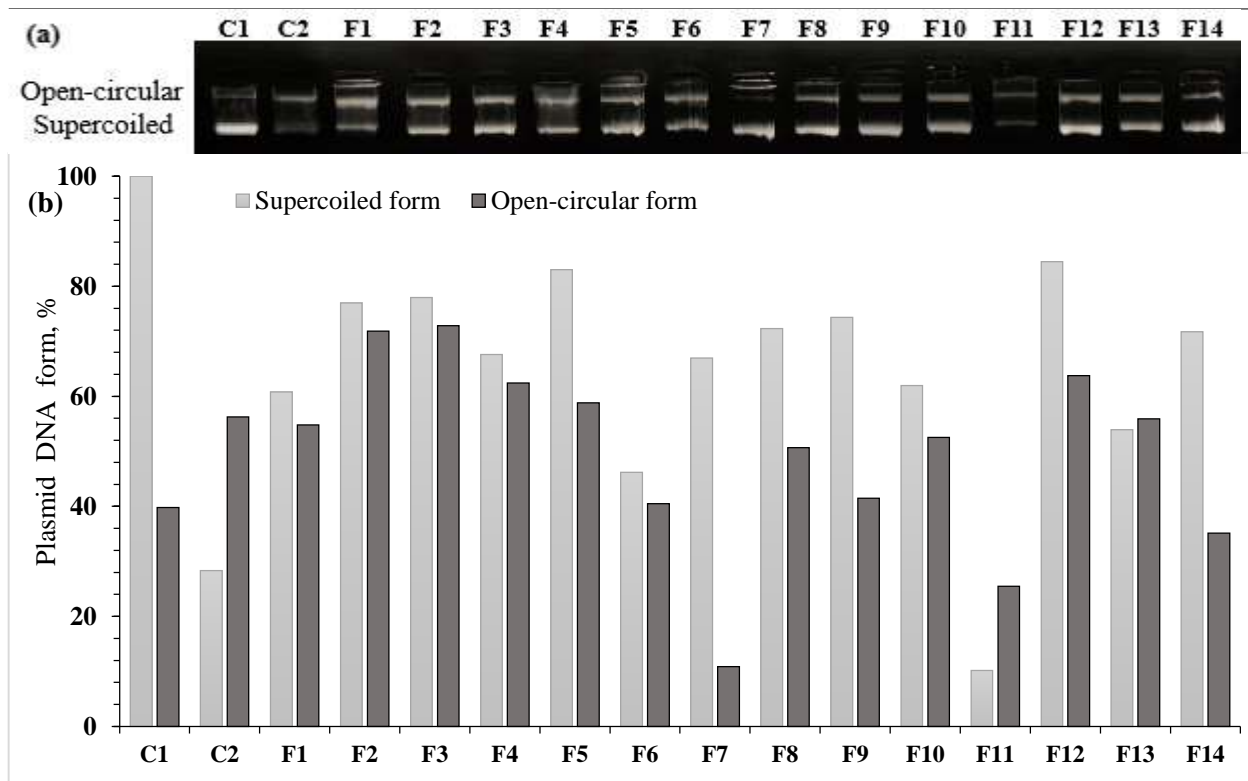


Figure 1. The results of DNA damage protection potential activities of *C. baskilensis* leaf fractions.

Şekil 1. *C. baskilensis* yaprak fraksiyonlarının DNA hasarı koruma potansiyel aktivitelerinin sonuçları

(a) DNA protection activity: Agarose gel electrophoresis image; lane 1: plasmid DNA as a positive control (C1), lane 2: plasmid DNA with H<sub>2</sub>O<sub>2</sub> and UV as a negative control (C2) and lane 3-23: plasmid DNA + H<sub>2</sub>O<sub>2</sub> + UV + different fraction samples. (b) Comparing chart of % density of the open-circular and supercoiled forms of plasmid DNA.

(a) DNA koruma aktivitesi: Agaroz jel elektroforezi görüntüsü; şerit 1: pozitif kontrol olarak plazmid DNA'sı (C1), şerit 2: negatif kontrol olarak H<sub>2</sub>O<sub>2</sub> ve UV içeren plazmid DNA'sı (C2) ve şerit 3-23: plazmid DNA + H<sub>2</sub>O<sub>2</sub> + UV + farklı fraksiyon örnekleri. (b) Plazmid DNA'sının açık dairesel ve süper sarmal formlarının % yoğunluk tablosunun karşılaştırılması.

### Principal component analysis (PCA)

The investigated dataset is made easier to understand by the principal component analysis. Multivariate analysis examines how the variables relate to the experimental groups and outliers. All fraction samples with enzyme inhibitory activities (1/IC<sub>50</sub>), antibacterial activity, and DNA protection activity were examined using Principal Component Analysis (PCA). The first two main components' eigenvalues were significant after PCA. The variance with enzyme inhibitions was 27.7% and 21.2% for the first component (PC1), the variance with antibacterial activity was 48.7% and 22.5% for the first component (PC1), and the variance with DNA protective activity was

75.3% and 24.7% for the first. F12 was positively correlated with AChE inhibition, *K. pneumoniae*, *B. cereus*, and *S. aureus* growth inhibition, and the supercoiled form protection of plasmid DNA according to a biplot graphic (Figure 2). We conclude that the F12 component is mostly the main reason behind the high bioactivity, which encourages us to do further fractionation to reach the pure compounds.

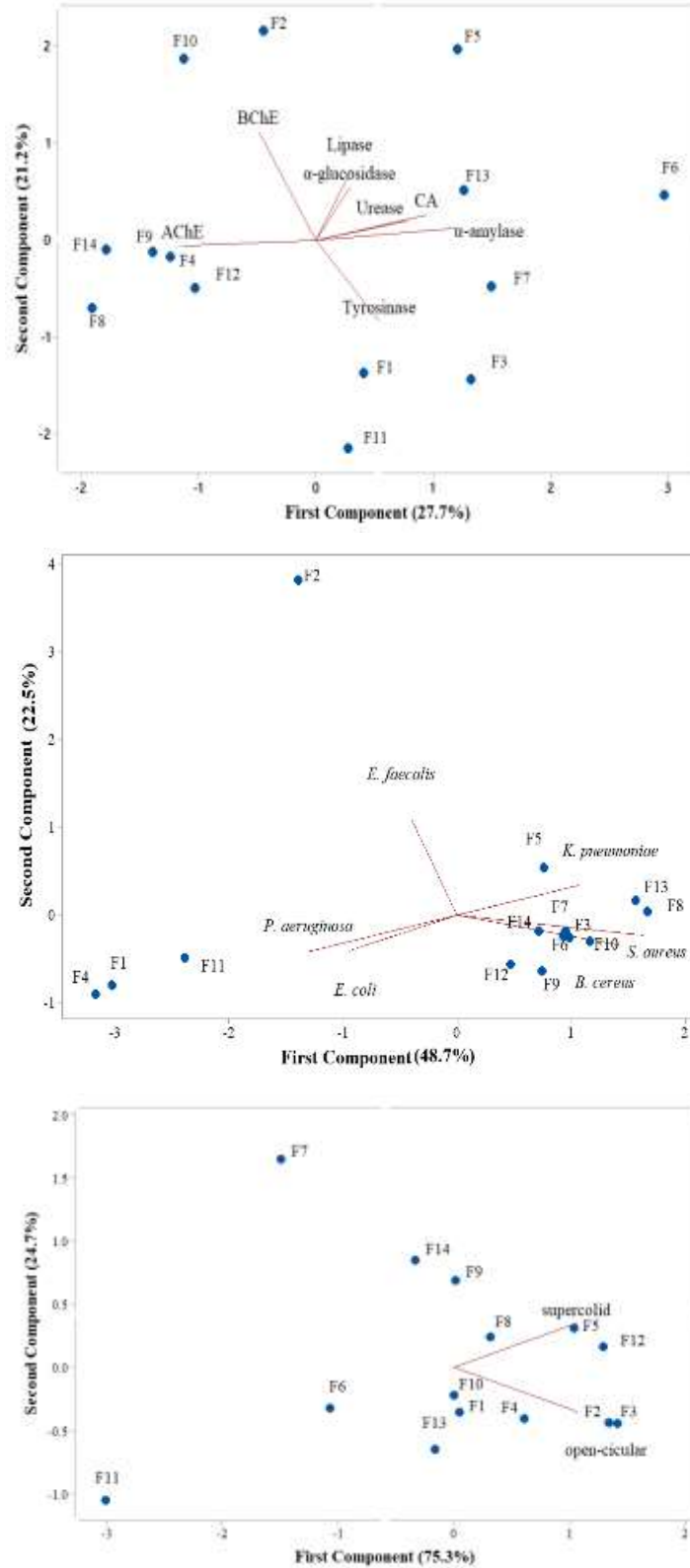


Figure 2. Biplot graph for PC1 and PC2 of fraction samples (F1-F14) with all activity results  
Şekil 2. Tüm aktivite sonuçlarıyla birlikte fraksiyon örneklerinin (F1-F14) PC1 ve PC2'sine ait Biplot grafiği

### Inositol isolation and characterization

*C. baskilensis* leaf fractions proved that it has high bioactivity in general; isolation of the leaf part and its detailed fractionation scheme are given in (Figure 3). At the end of this study, bioactive molecules had been isolated from the leaf part of *C. baskilensis*. The structures of isolated molecules were determined spectroscopically using NMR.

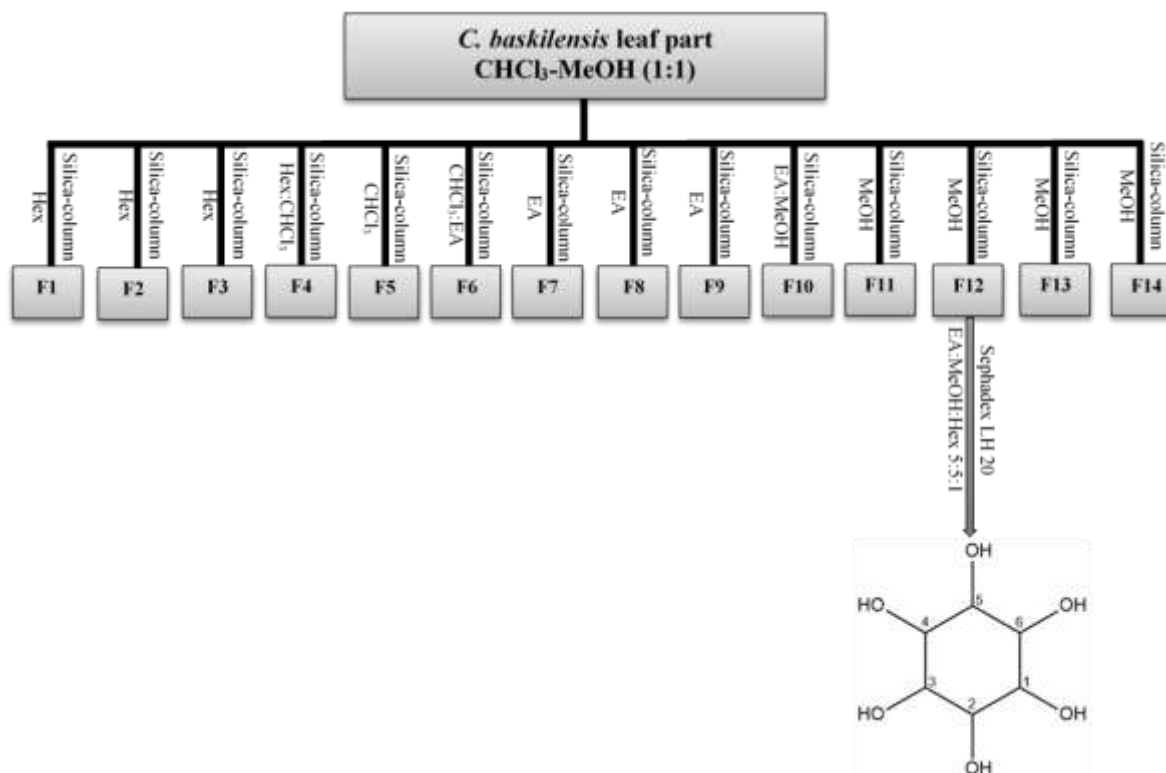


Figure 3. Fractionation scheme of *C. baskilensis* leaf  
Şekil 3. *C. baskilensis* yaprağının fraksiyonlama şeması

Since the F12 fraction was highly active in many bioassays, the chromatographic isolation sub-fractionation process led to isolating a colorless cubic crystalline material. This isolated metabolite was dissolved with DMSO, and its structure was investigated using H-NMR spectroscopy. The structure of the isolated compound was identified through NMR spectra as a carbocyclic sugar inositol, and its structure was compatible with the literature data. H-NMR and C13-NMR spectra belonging to the inositol compound have been clarified in (Figure 4-Figure 7, Table 3) In his study by Dzhumyrko and Shinkarenko (1971), a molecular substance with an inositol structure was isolated from *C. oblongifolia* leaf ethanol extract by fractional crystallization, and the mineral was defined as L-inositol. Another study by Nikolova et al. (2019) that was related to the analysis of the metabolite profiles of *C. lanata*, one of the endemic plants of the Balkans, inositol, had been identified and isolated as a result of this study.

Table 3. H-NMR and <sup>13</sup>C-NMR spectrum data of the inositol molecule

Çizelge 3. İnositol molekülünün H-NMR ve <sup>13</sup>C-NMR spektrum verileri

Carbon No.	H-NMR (600 MHz, DMSO d6)	C13-NMR (150 MHz, CDC13 d-1 d)	H-NMR (270MHz, DMSO d6)(Salazar-Pereda et al., 1997)	<sup>13</sup> C13-NMR (67.8 MHz)(Salazar-Pereda et al., 1997)
1	3.10	72.32	3.10 (ddd)	72.01
2	3.68	73.08	3.68 (td)	72.79
3	3.10	72.32	3.10 (ddd)	72.01
4	3.31	73.21	3.32 (ddd)	72.91
5	2.89	75.69	2.88 (ddd)	75.38
6	3.31	73.21	3.32 (ddd)	72.91

Inositol isomers were investigated in a previous study on *Campanula* species. The *C. elator*, *C. taurica*, and *C. hohenaceri* species were extracted using hot water and then extracted using ethyl acetate. The resulting precipitate was extracted and crystallized in an ethanol-water mixture after the obtained ethyl acetate extract was

concentrated and chloroform was added. The assays conducted revealed that the crystals were meso-inositol (Dzhumyrko and Shinkarenko, 1972).

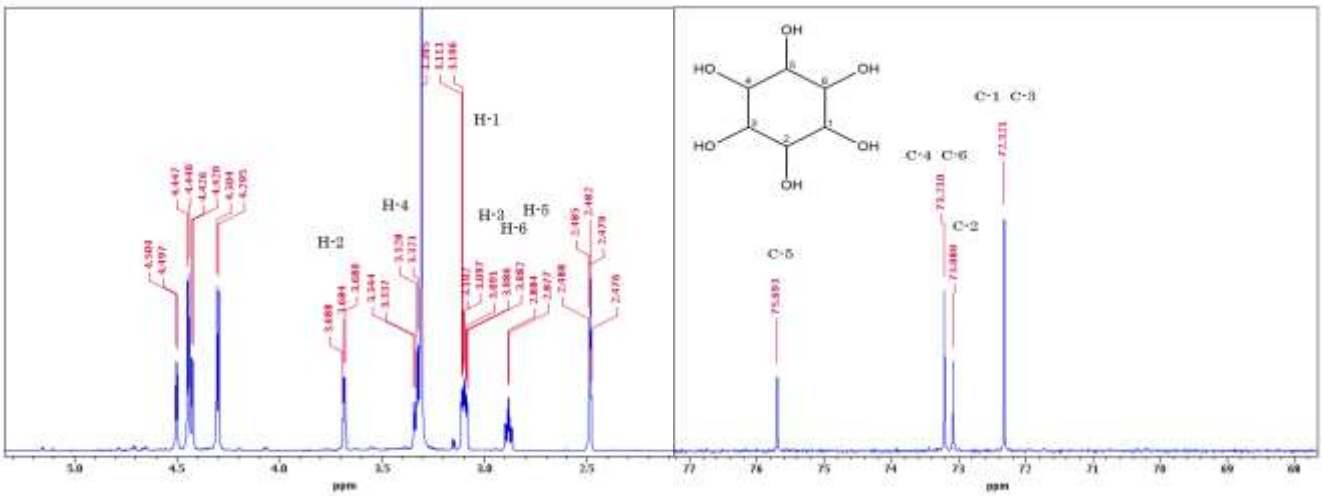


Figure 4. H-NMR and C13-NMR spectra of the inositol molecule  
*Şekil 4. Inositol molekülünün H-NMR ve C13-NMR spektrumları*

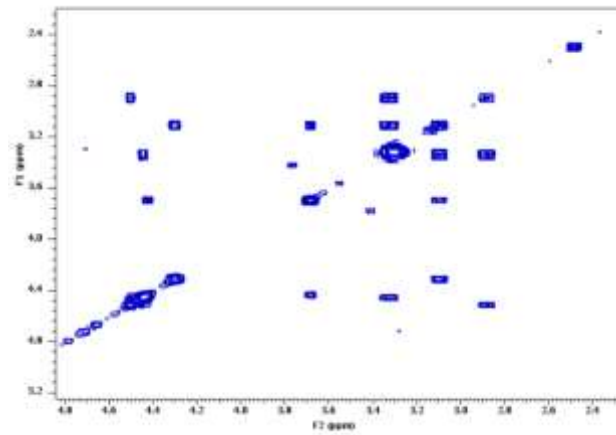


Figure 5. COSY-NMR spectrum of the inositol molecule  
*Şekil 5. Inositol molekülünün COSY-NMR spektrumu*

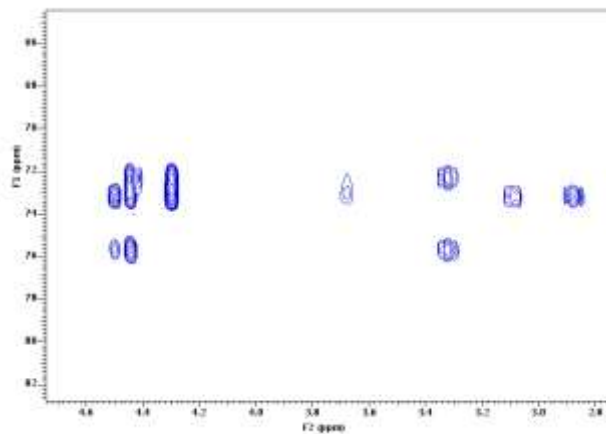


Figure 6. HMBC-NMR spectrum of the inositol molecule  
*Şekil 6. Inositol molekülünün HMBC-NMR spektrumu*

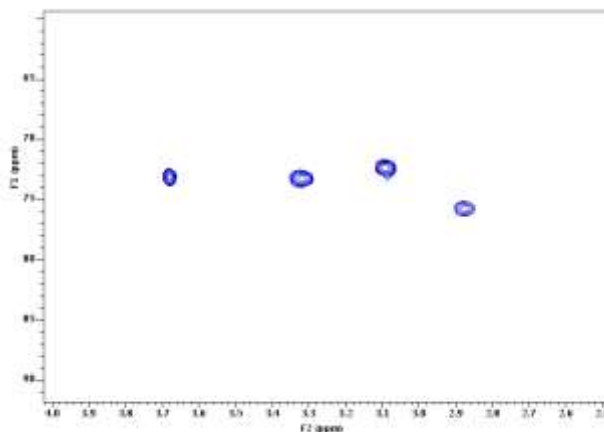


Figure 7. HSQC NMR spectrum of the inositol molecule  
 Şekil 7. İnositol molekülünün HSQC NMR spektrumu

### Molecular Docking and Molecular Dynamics

We theoretically investigated the molecular interaction between inositol and the standard inhibitor (galantamine) and the most inhibited enzyme to sketch a potential mechanism for AChE inhibition brought on by F12 against the enzymes examined *in vitro*; also for comparison, we investigated the molecular interaction between inositol and the standard inhibitor with BChE, being from the same category and sharing a similar function. It is worth noting that the theoretical interaction results were consistent with the practical inhibition results for both enzymes. The binding energy of the enzyme-inositol interaction is -6.1 kcal/mol. Seven interactions were found by molecular docking between the isolated molecule and acetylcholine esterase: a carbon-hydrogen bond with PRO410 residue, three conventional hydrogen bonds with ASN233, two with ASN533, and the final one with GLU313 residue. Nine interactions formed between galantamine and AChE: two conventional hydrogen bonds with SER239 residue; two carbon-hydrogen bonds with SER239 and TYR124 residues, two pi-pi stacked hydrophobic interactions with TRP286 residue; a pi-pi T-shaped hydrophobic interaction with TYR72 residue; two pi-alkyl hydrophobic interactions with TYR72 and TRP286 residues. The interaction between inositol and BChE consisted of a single conventional hydrogen bond between the molecule and GLN498 residue. Four interactions formed between galantamine and BChE: a carbon-hydrogen bond with ASN83 residue, pi-pi stacked hydrophobic interaction with TRP82 residue; two pi-alkyl hydrophobic interactions with TRP82 residue (Table 4, Figure 8).

Table 4. Molecule docking scores between inositol and galantamine with AChE and BChE  
 Çizelge 4. AChE ve BChE ile inositol ve galantamine arasındaki molekül doking skor

Compound	Binding energy (kcal/mol)	
	AChE	BChE
Inositol	-6.1	-5.7
Galantamine	-8.3	-9.0

Considering the result of molecular docking, we tested the kinetics and stability via the molecular dynamics of each isolated compound and compared it with the reference material against AChE as the highly inhibited enzyme. Greater RMSDs suggested that the backbone had structural changes over the simulation period, whereas smaller RMSD values suggested that the protein was highly stable. Over 100 ns, the inositol-AChE complex changed by about 5 nm (Figure 9). Throughout the simulation, the root mean square fluctuation (RMSF) method is used to compute the changes in each amino acid residue with and without specific ligand molecules. Using the Ca atoms of AChE, the RMSF was computed for all complex systems and revealed that the fluctuation intensity persisted between 0.05-0.35 nm (Figure 9). To determine the stability during the MD simulations, it was essential to examine the bonding interactions between ligands and proteins (Majewski et al., 2019).

Figure 9 depicts the H-bond that formed between inositol and AChE throughout 100 ns. Throughout the MD simulation, there was continuous interaction around five bonds, which most likely contributed to the stability of this interaction. A protein's radius of gyration (Rg) indicates its degree of compactness. Rg is a practical and reliable indicator of a drug's capacity to alter protein structure. The Rg value of a protein indicates its loose molecular

packing. The dynamics computation for 100 ns showed that AChE and inositol were constant at less than 2.35 nm (Figure 9).

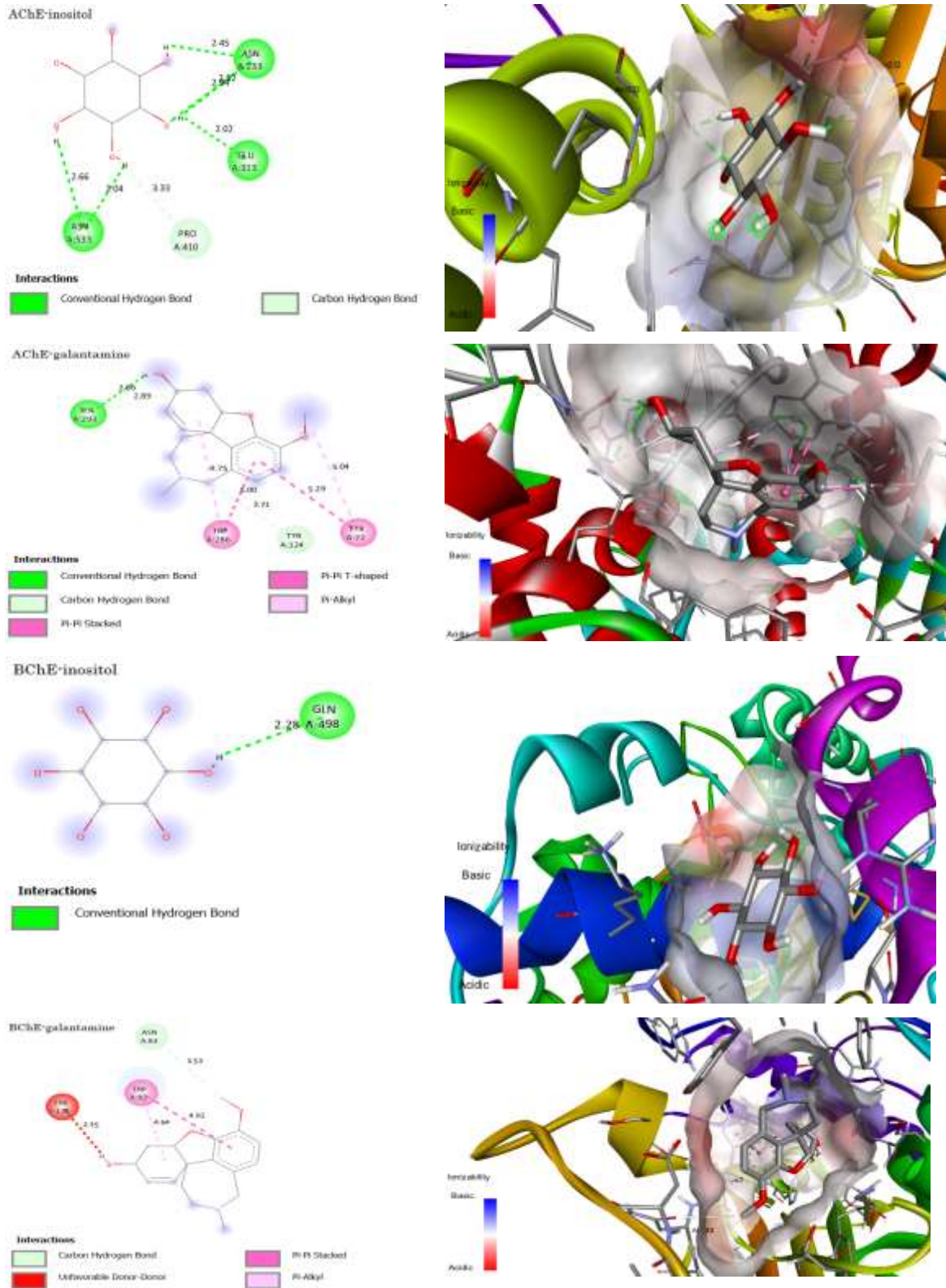


Figure 8. Molecule docking interaction between inositol and galantamine with AChE and BChE  
*Şekil 8. Inositol ve galantamine ile AChE ve BchE arasındaki molekül doking etkileşimi*

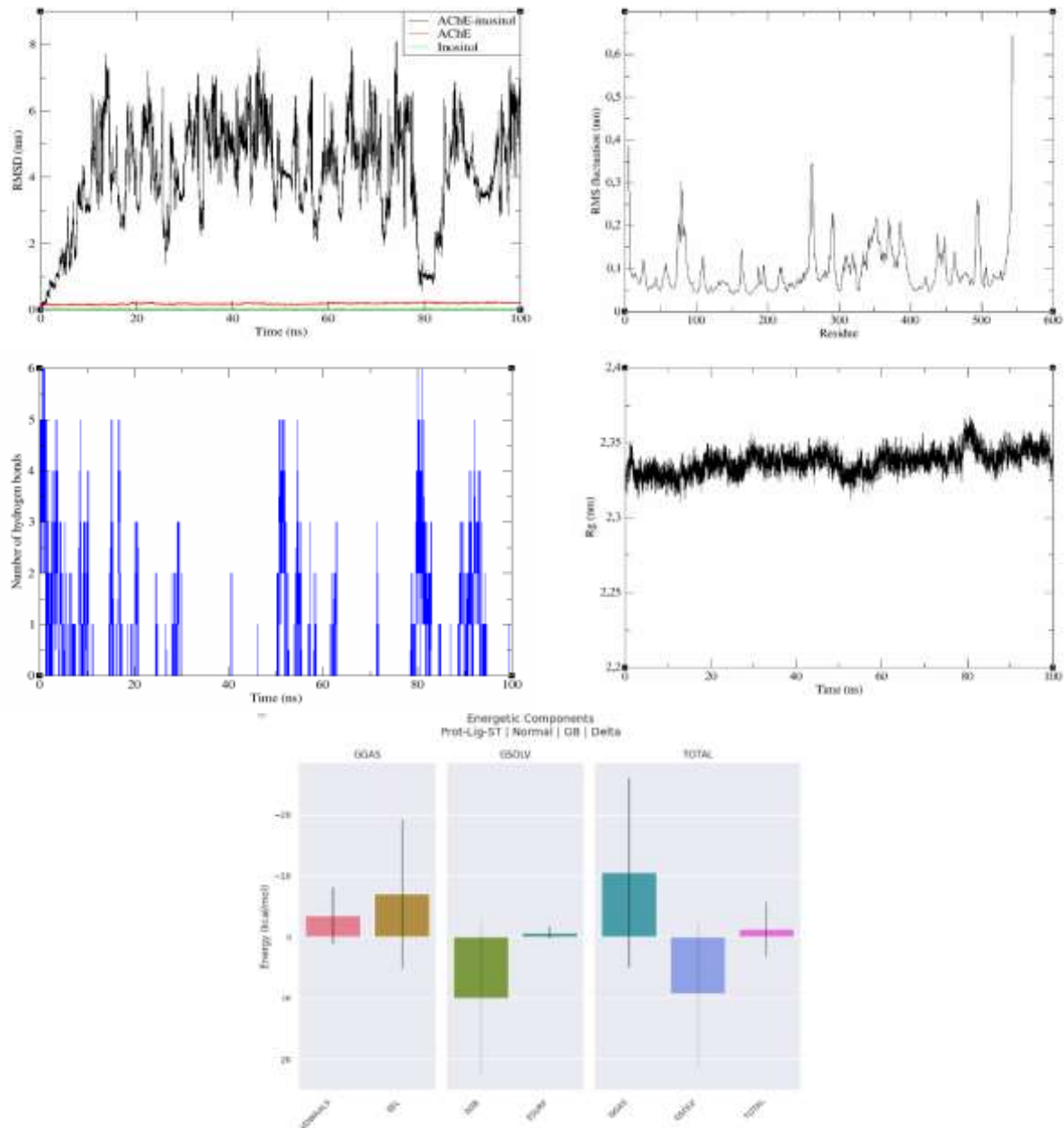


Figure 9. Molecular dynamic simulation results between inositol and AChE for 100 ns, RMSD, RMSF, time-dependent H-bond interactions, Rg plotting, Gmx\_mmpbsa energy of Delta.

Şekil 9. İnoSitol ve AChE arasındaki 100 ns'lik moleküler dinamik simülasyon sonuçları, RMSD, RMSF, zamana bağlı H-bağı etkileşimleri, Rg çizimi, Delta'nın Gmx\_mmpbsa enerjisi.

On the other hand, the RMSD for the galantamine-AChE complex changed by about 0.5 nm. In contrast, the RMSF was computed for all complex systems and revealed that the fluctuation intensity persisted between 0.05 and 0.4 nm. H-bond that formed between galantamine and AChE throughout 100 ns was a continuous interaction around 2-3 bonds, which most likely contributed most to the stability of this interaction. Rg value of a protein indicates its loose molecular packing, for 100 ns showed that AChE and galantamine were constant between 2.3-2.35 nm (Figure 10).

The formula  $\Delta G_{\text{binding}} = G_{\text{complex}} - (G_{\text{receptor}} + G_{\text{ligand}})$  was used to calculate the binding energy ( $\Delta G_{\text{binding}}$ ) of the protein-ligand system, where  $G_{\text{receptor}}$  stands for the binding energy of AChE and  $G_{\text{ligand}}$  for the energy of the unbounded ligand.  $\Delta G_{\text{binding}}$  can also be expressed as follows: When  $\Delta H$  is the binding enthalpy and  $-\Delta S$  is the conformational entropy after ligand binding, the formula is  $\Delta G_{\text{binding}} = \Delta H - T\Delta S$ . For comparing relative binding free energies for similar systems, the approximated value—the effective free energy when the entropic factor is taken out—is usually adequate. This analysis discovered that the average effective free energy of binding

was  $-1.32 \pm 3.79$  kcal/mol for inositol and  $-11.92 \pm 0.02$  kcal/mol for galantamine (Table 5, Figures 9 and 10). Following the docking data, MMPBSA simulations indicated a stable interaction of the inositol molecule with the AChE.

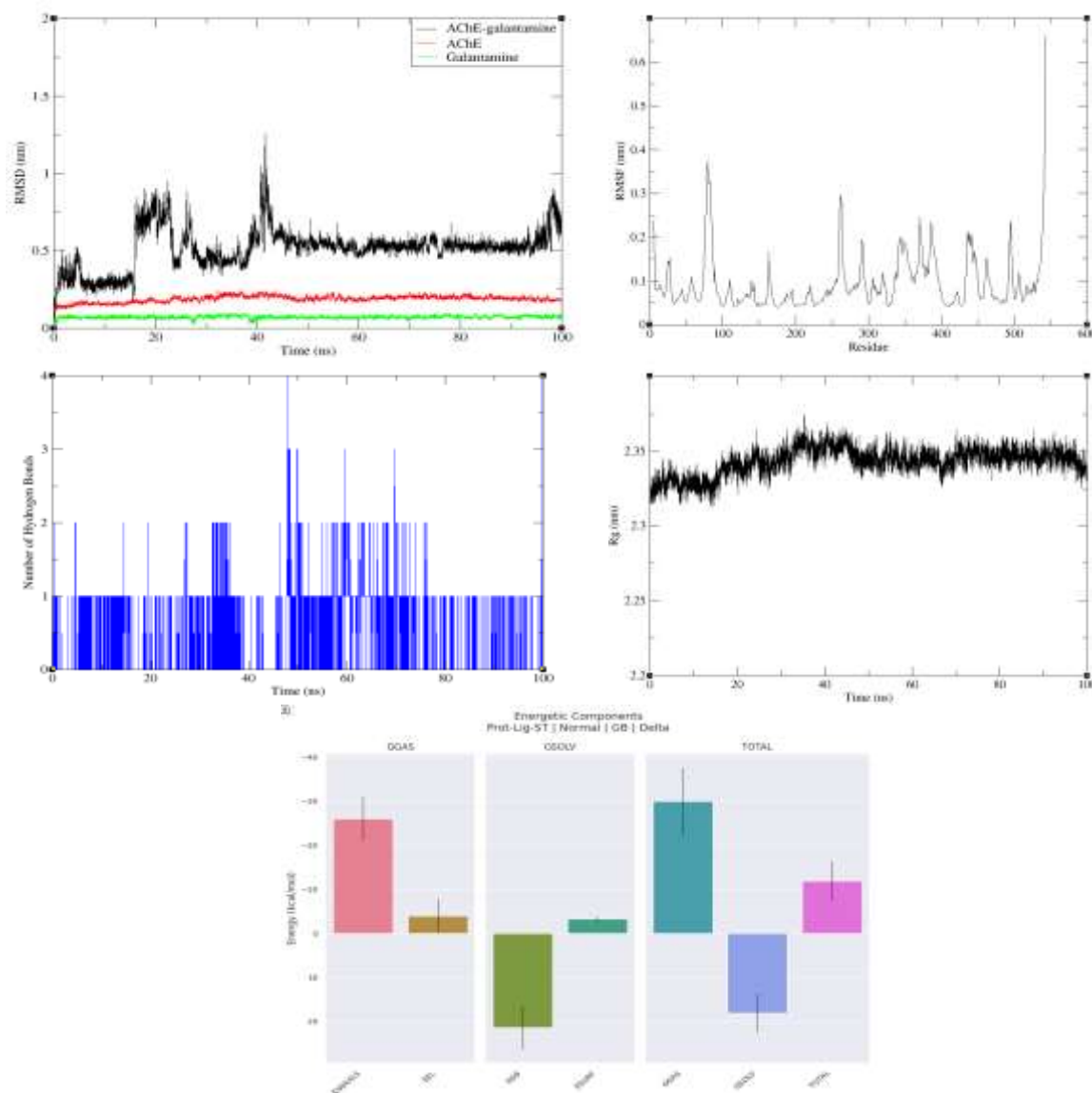


Figure 10. Molecular dynamic simulation results between galantamine and AChE for 100 ns, RMSD, RMSF, time-dependent H-bond interactions, Rg plotting, Gmx\_mmpbsa energy of Delta.

Şekil 10. Galantamine ve AChE arasındaki 100 ns'lik moleküler dinamik simülasyon sonuçları, RMSD, RMSF, zamana bağlı H-bağı etkileşimleri, Rg çizimi, Delta'nın Gmx\_mmpbsa enerjisi.

## CONCLUSION

Isolation was applied to reach the active compounds of the *C. baskilensis* leaf part. The fractionation process led to the obtaining of 14 different fractions in the first part. Numerous *in-vitro* bioassays have been applied to investigate the bioactivity of fractions, antibacterial, enzyme inhibition, and DNA-related assays. The results of these assays proved that many of the tested fraction samples had high biological effectiveness. All obtained activity results have been compared with standard antibiotics and standard inhibition drugs. The results were compared with the studies with the same biological activity tests in the literature. The principal component analysis leads us to conclude that the F12 component is primarily responsible for the high activity examined in this study, which was the subject of the second fractionation. As a result, pure compounds were obtained when the isolation of the fractions with the highest effectiveness was applied. The structure of the isolated compound was clarified using the NMR spectroscopic technique. The isolated compound was identified as inositol. We decided to move forward with exposing the inhibitory mechanism for the isolated compound against the more inhibited enzyme by F12; we tested this isolated compound and galantamine theoretically by simulating molecular docking in a vacuum via molecular docking and also made an advanced simulation about the stability of the complex for 100 ns under the

standard conditions of the living organism. It became clear that this compound can form a relatively stable association due to its formation of many hydrogen bonds, as proven by the study of molecular dynamics and energy calculations. Ultimately, taking this path may also allow us to discover the true capabilities of the compounds that isolate and test them *in silico* and *in vitro*.

Table 5. Free energy of binding obtained using MMPBSA calculations (Complex:Receptor-Ligand)  
*Çizelge 5 MMPBSA hesaplamaları kullanılarak elde edilen bağlanma serbest enerjisi (Kompleks:Reseptör-Ligand)*

Energy Component	Average	
	AChE*	BChE*
ΔBOND	-0.00±0.00	-0.00±0.05
ΔANGLE	0.00±0.00	0.00±0.07
ΔDIHED	0.00±0.00	-0.00±0.05
ΔUB	-0.00±0.00	0.00±0.01
ΔIMP	0.00±0.00	0.00±0.00
ΔCMAP	0.00±0.00	0.00±0.00
ΔVDWAALS	-3.51±0.09	-26.00±0.01
ΔEEL	-7.05±0.24	-4.02±0.01
Δ1-4 VDW	-0.00±0.00	-0.00±0.03
Δ1-4 EEL	0.00±0.00	-0.00±0.03
ΔEGB	9.98±0.25	21.36±0.00
ΔESURF	-0.73±0.02	-3.25±0.00
ΔGGAS	-10.56±0.31	-30.03±0.02
ΔGSOLV	9.25±0.24	18.10±0.00
ΔTOTAL	-1.32±0.09	-11.92±0.02

\*Values are mean±standard error, kcal/mol

## ACKNOWLEDGMENTS

The authors thank the Office of Scientific Research Projects Coordination at Ondokuz Mayıs University, grant number PYO.FEN.1904.20.003.

## Contribution Rate Statement Summary of Researchers

The authors declare that they have contributed equally to the article.

## Conflict of Interest

The authors declare that they have no known competing financial interests or personal relationships that could have appeared to influence the work reported in this paper.

## REFERENCES

- Abraham, M.J., Murtola, T., Schulz, R., Páll, S., Smith, J.C., Hess, B., Lindahl, E., 2015. GROMACS: High performance molecular simulations through multi-level parallelism from laptops to supercomputers. *SoftwareX* 1, 19-25.
- Addar, L., Bensouici, C., Zennia, S.S.A., Haroun, S.B., Mati, A., 2019. Antioxidant, tyrosinase, and urease inhibitory activities of camel αS-casein and its hydrolysate fractions. *Small Ruminant Research*, 173, 30-35. <https://doi.org/10.1016/j.smallrumres.2019.01.015>.
- Akkoc, S., Karatas, H., Muhammed, M.T., Kökbudak, Z., Ceylan, A., Almalki, F., Laaroussi, H., Ben Hadda, T., 2023. Drug design of new therapeutic agents: Molecular docking, molecular dynamics simulation, DFT and POM analyses of new Schiff base ligands, and impact of substituents on bioactivity of their potential antifungal pharmacophore site. *Journal of Biomolecular Structure and Dynamics*, 41 (14), 6695-6708.
- Alcítepe, E., 2011. New combinations in Campanula sect. Quinqueloculares from Turkey. *Pakistan Journal of Botany*, 43 (5), 2243-2254.
- Baiseitova, A., Jenis, J., Kim, J.Y., Li, Z.P., Park, K.H., 2021. Phytochemical analysis of the aerial part of *Ikonnikovia kaufmanniana* and their protection of DNA damage. *Natural Product Research*, 35 (5), 880-883. <https://doi.org/10.1080/14786419.2019.1607858>
- Başar, Y., Demirtaş, İ., Yenigün, S., İpek, Y., Özen, T., Behçet, L., 2024. Molecular docking, molecular dynamics, MM/PBSA approaches and bioactivity studies of nepetanudoside B isolated from endemic *Nepeta aristata*. *Journal of Biomolecular Structure and Dynamics*, 1-14. <https://doi.org/10.1080/07391102.2024.2309641>.

- Behçet, L., İlçim, A., 2018. *Campanula baskilensis* sp. nov. (Campanulaceae), a new chasmophyte from Turkey with unusual capsule dehiscence. *Nordic Journal of Botany*, 36 (10), e01940. <https://doi.org/10.1111/njb.01940>.
- Berman, H.M., Westbrook, J., Feng, Z., Gilliland, G., Bhat, T.N., Weissig, H., Shindyalov, I.N., Bourne, P.E., 2000. The protein data bank. *Nucleic Acids Research* 28 (1), 235-242. <https://doi.org/10.1093/nar/28.1.235>.
- Bernhoft, A., 2010. A brief review on bioactive compounds in plants. *Bioactive Compounds in Plants: Benefits and Risks for Man and Animals*, 50, 11-17.
- BIOVIA, D.S., 2017. BIOVIA Discovery Studio Visualizer. Software version 20, 779.
- Bjellmar, P., Larsson, P., Cuendet, M.A., Hess, B., Lindahl, E., 2010. Implementation of the CHARMM force field in GROMACS: analysis of protein stability effects from correction maps, virtual interaction sites, and water models. *Journal of Chemical Theory and Computation*, 6 (2), 459-466.
- Brandt, K., Dötterl, S., Francke, W., Ayasse, M., Milet-Pinheiro, P., 2017. Flower Visitors of *Campanula*: Are Oligoleges More Sensitive to Host-Specific Floral Scents Than Polyleges? *Journal of Chemical Ecology*, 43 (1), 4-12.
- Bucar, F., Wube, A., Schmid, M., 2013. Natural product isolation—how to get from biological material to pure compounds. *Natural Product Reports*, 30 (4), 525-545.
- Chanda, J., Mukherjee, P.K., Biswas, R., Biswas, S., Tiwari, A.K., Pargaonkar, A., 2019. UPLC-QTOF-MS analysis of a carbonic anhydrase-inhibiting extract and fractions of *Luffa acutangula* (L.) Roxb (ridge gourd). *Phytochemical Analysis*, 30 (2), 148-155. <https://doi.org/10.1002/pca.2800>.
- Cuendet, M., Potterat, O., Hostettmann, K., 2001. Flavonoids and phenylpropanoid derivatives from *Campanula barbata*. *Phytochemistry*, 56 (6), 631-636.
- Dillard, C.J., German, J.B., 2000. Phytochemicals: nutraceuticals and human health. *Journal of the Science of Food and Agriculture*, 80 (12), 1744-1756.
- Dumlu, M., Gurkan, E., Tuzlaci, E., 2008. Chemical composition and antioxidant activity of *Campanula alliariifolia*. *Natural Product Research*, 22 (6), 477-482. <https://doi.org/10.1080/14786410701640429>.
- Dzhumyrko, S., Shinkarenko, A., 1971. L-inositol from *Campanula oblongifolia*. *Chemistry of Natural Compounds*, 7 (5), 638-638.
- Dzhumyrko, S., Shinkarenko, A., 1972. Mesoinositol from some species of the genus *Campanula*. *Chemistry of Natural Compounds*, 8 (3), 374-375.
- Ellman, G.L., Courtney, K.D., Andres Jr, V., Featherstone, R.M., 1961. A new and rapid colorimetric determination of acetylcholinesterase activity. *Biochemical Pharmacology*, 7 (2), 88-95. [https://doi.org/10.1016/0006-2952\(61\)90145-9](https://doi.org/10.1016/0006-2952(61)90145-9).
- Ercan, P., El, S.N., 2016. Inhibitory effects of chickpea and *Tribulus terrestris* on lipase,  $\alpha$ -amylase and  $\alpha$ -glucosidase. *Food Chemistry*, 205, 163-169. <https://doi.org/10.1016/j.foodchem.2016.03.012>.
- Harvey, A., 2000. Strategies for discovering drugs from previously unexplored natural products. *Drug Discovery Today*, 5 (7), 294-300.
- Hassanien, M., El-Shamy, H., Ghany, A.A., 2014. Characterization of fatty acids, bioactive lipids, and radical scavenging activity of Canterbury bells seed oil. *Grasas y Aceites*, 65 (2), e019. <https://doi.org/10.3989/gya.074413>.
- Ishida, S., Okasaka, M., Ramos, F., Kashiwada, Y., Takaishi, Y., Kodzhimatov, O.K., Ashurmetov, O., 2008. New alkaloid from the aerial parts of *Codonopsis clematidea*. *Journal of Natural Medicines*, 62 (2), 236-238.
- Kim, H.-J., Son, D.C., Kim, H.-J., Choi, K., Oh, S.-H., Kang, S.-H., 2017. The chemotaxonomic classification of Korean Campanulaceae based on triterpene, sterol, and polyacetylene contents. *Biochemical Systematics and Ecology*, 74, 11-18. <https://doi.org/10.1016/j.bse.2017.07.002>.
- Kim, H.-Y., Lim, S.-H., Park, Y.-H., Ham, H.-J., Lee, K.-J., Park, D.-S., Kim, K.-H., Kim, S.-M., 2011. Screening of  $\alpha$ -amylase,  $\alpha$ -glucosidase and lipase inhibitory activity with Gangwon-do wild plants extracts. *Journal of the Korean Society of Food Science and Nutrition*, 40 (2), 308-315.
- Kim, J.Y., Hwang, Y.P., Kim, D.H., HAN, E.H., Chung, Y.C., Roh, S.H., Jeong, H.G., 2006. Inhibitory effect of the saponins derived from roots of *Platycodon grandiflorum* on carrageenan-induced inflammation. *Bioscience, Biotechnology, and Biochemistry*, 70 (4), 858-864.
- Korkmaz, B., Fandakli, S., Barut, B., Yildirim, S., Sener, S.O., Ozturk, E., Terzioglu, S., Yayli, N., 2020. Volatile and Phenolic Components and Antioxidant, Acetylcholinesterase, Tyrosinase,  $\alpha$ -Glucosidase Inhibitory Effects of Extracts Obtained From *Campanula latifolia* L. subsp. *latifolia*. *Journal of Essential Oil Bearing Plants*, 23 (5), 1118-1131.
- Lammers, T.G., 2007. World checklist and bibliography of Campanulaceae, Campanulaceae. Royal Botanic Gardens, Kew, p. 675.
- Liu, R.H., 2004. Potential synergy of phytochemicals in cancer prevention: mechanism of action. *The Journal of Nutrition*, 134 (12), 3479S-3485S.

- Majewski, M., Ruiz-Carmona, S., Barril, X., 2019. An investigation of structural stability in protein-ligand complexes reveals the balance between order and disorder. *Communications Chemistry* 2(1), 110.
- Malviya, N., Malviya, S., 2017. Bioassay guided fractionation-an emerging technique influence the isolation, identification and characterization of lead phytomolecules. *Hosp. Pharm*, 2(5), 1-6.
- Marah, S., Ipek, Y., Gul, F., Demirtas, I., Behcet, L., Ozen, T., 2024. Phytochemical profiles, bioactivities, and molecular docking and molecular dynamics approaches of endemic *Campanula baskilensis* Behçet (campanulaceae). *Journal of the Indian Chemical Society*, 101(11), 101358.
- Mayur, B., Sancheti, S., Shruti, S., Sung-Yum, S., 2010. Antioxidant and-glucosidase inhibitory properties of *Carpesium abrotanoides* L. *Journal of Medicinal Plants Research*, 4 (15), 1547-1553. <https://doi.org/10.5897/JMPR.9000218>.
- McDougall, G.J., Kulkarni, N.N., Stewart, D., 2009. Berry polyphenols inhibit pancreatic lipase activity in vitro. *Food Chemistry*, 115(1), 193-199. <https://doi.org/10.1016/j.foodchem.2008.11.093>.
- Nastić, N., Švarc-Gajić, J., Delerue-Matos, C., Barroso, M.F., Soares, C., Moreira, M.M., Morais, S., Mašković, P., Srček, V.G., Slivac, I., 2018. Subcritical water extraction as an environmentally-friendly technique to recover bioactive compounds from traditional Serbian medicinal plants. *Industrial Crops and Products* 111, 579-589.
- Newman, D.J., Cragg, G.M., 2016. Natural products as sources of new drugs from 1981 to 2014. *Journal of Natural Products*, 79(3), 629-661.
- Nikolova, M., Aneva, I., Zhelev, P., Berkov, S., 2019. GC/MS Based Metabolite Profiling and Antioxidant Activity of Balkan and Bulgarian Endemic Plants. *Agriculturae Conspectus Scientificus*, 84(1), 59-65.
- Ouzounis, T., Fretté, X., Rosenqvist, E., Ottosen, C.-O., 2014. Spectral effects of supplementary lighting on the secondary metabolites in roses, chrysanthemums, and campanulas. *Journal of Plant Physiology*, 171(16), 1491-1499. <https://doi.org/10.1016/j.jplph.2014.06.012>.
- Qi, Y., Choi, S.-I., Son, S.-R., Han, H.-S., Ahn, H.S., Shin, Y.-K., Lee, S.H., Lee, K.-T., Kwon, H.C., Jang, D.S., 2020. Chemical constituents of the leaves of *Campanula takesimana* (Korean Bellflower) and their inhibitory effects on LPS-induced PGE2 production. *Plants*, 9(9), 1232.
- Rameau, J.-C., Mansion, D., Dumé, G., 1989. Flore forestière française: guide écologique illustré. Montagnes. Forêt privée française, France, 87-97.
- Reller, L.B., Weinstein, M., Jorgensen, J.H., Ferraro, M.J., 2009. Antimicrobial susceptibility testing: a review of general principles and contemporary practices. *Clinical Infectious Diseases*, 49 (11), 1749-1755. <https://doi.org/10.1086/647952>.
- Russo, A., Izzo, A.A., Borrelli, F., Renis, M., Vanella, A., 2003. Free radical scavenging capacity and protective effect of *Bacopa monniera* L. on DNA damage. *Phytotherapy Research: An International Journal Devoted to Pharmacological and Toxicological Evaluation of Natural Product Derivatives*, 17 (8), 870-875. <https://doi.org/10.1002/ptr.1061>.
- Salazar-Pereda, V., Martínez-Martínez, F.J., Contreras, R., Flores-Parra, A., 1997. NMR and X-ray diffraction study of some inositol derivatives. *Journal of Carbohydrate Chemistry* 16(9), 1479-1507.
- Sancheti, S., Sancheti, S., Seo, S.-Y., 2010. Evaluation of antiglycosidase and anticholinesterase activities of *Boehmeria nivea*. *Pakistan Journal of Pharmaceutical Sciences*, 23(2), 236-240.
- Sarker, S.D., Nahar, L., 2012. An introduction to natural products isolation. *Natural Products Isolation*, 1-25.
- Sevgi, K., Tepe, B., Sarikurkcu, C., 2015. Antioxidant and DNA damage protection potentials of selected phenolic acids. *Food and Chemical Toxicology*, 77, 12-21. <https://doi.org/10.1016/j.fct.2014.12.006>.
- Sinek, K., Iskender, N.Y., YAYLI, N., 2012. Antimicrobial Activity and Chemical Composition of the Essential Oil from *Campanula glomerata* L. Subsp. *Hispida* (Witasek) Hayek. *Asian Journal of Chemistry* 24 (5), 1931-1934.
- Singh, D., Chaudhuri, P.K., 2018. A review on phytochemical and pharmacological properties of Holy basil (*Ocimum sanctum* L.). *Industrial Crops and Products*, 118, 367-382.
- Tepe, B., Degerli, S., Arslan, S., Malatyali, E., Sarikurkcu, C., 2011. Determination of chemical profile, antioxidant, DNA damage protection and antiamebic activities of *Teucrium polium* and *Stachys iberica*. *Fitoterapia*, 82(2), 237-246. <https://doi.org/10.1016/j.fitote.2010.10.006>
- Trentin, R., Custódio, L., Rodrigues, M.J., Moschin, E., Sciuto, K., da Silva, J.P., Moro, I., 2020. Exploring *Ulva australis* Areschoug for possible biotechnological applications: In vitro antioxidant and enzymatic inhibitory properties, and fatty acids contents. *Algal Research*, 50, 101980. <https://doi.org/10.1016/j.algal.2020.101980>.
- Trott, O., Olson, A.J., 2010. AutoDock Vina: improving the speed and accuracy of docking with a new scoring function, efficient optimization, and multithreading. *Journal of Computational Chemistry*, 31(2), 455-461.
- Valdés-Tresanco, M.S., Valdés-Tresanco, M.E., Valiente, P.A., Moreno, E., 2021. gmx\_MMPBSA: a new tool to perform end-state free energy calculations with GROMACS. *Journal of Chemical Theory and Computation*, 17(10), 6281-6291.
- Vergauwen, R., Van den Ende, W., Van Laere, A., 2000. The role of fructan in flowering of *Campanula rapunculoides*. *Journal of Experimental Botany*, 51(348), 1261-1266.

- Vincken, J.-P., Heng, L., de Groot, A., Gruppen, H., 2007. Saponins, classification and occurrence in the plant kingdom. *Phytochemistry*, 68 (3), 275-297.
- Yildirim, H., 2018. *Campanula leblebicii* (Campanulaceae), a new chasmophyte species from western Turkey. *Phytotaxa*, 376 (2), 114-122.
- Zarei, M.A., Tahazadeh, H., 2020. Alpha-glucosidase Inhibitory Activity in Methanol Extract of some Plants from Kurdistan Province. *Journal of Medicinal Plants*, 4 (72), 227-235.
- Zhang, L., Mulrooney, S.B., Leung, A.F., Zeng, Y., Ko, B.B., Hausinger, R.P., Sun, H., 2006. Inhibition of urease by bismuth (III): implications for the mechanism of action of bismuth drugs. *Biometals*, 19 (5), 503-511. <https://doi.org/10.1007/s10534-005-5449-0>.